Ongoing Studies for Automatic Road Anomalies Detection on 2D and 3D Pavement Images

W Kaddah, Marwa El Bouz, Yousri Ouerhani, Ayman Alfalou, Marc Desthieux

Ongoing Studies for Automatic Road Anomalies Detection on 2D and 3D Pavement Images

Wissam Kaddah[1,2], Marwa Elbouz[2], Yousri Ouerhani[1], Ayman Alfalou[2] and Marc Desthieux[1]

[1] Actris, BP 30143, 29803 Brest Cedex 9, France
[2] ISEN-Brest, Vision Lab., L@bISEN, CS 42807, 29228 Brest Cedex 2, France

ABSTRACT

A pavement is a solid surface material laid down on an area intended to support foot and vehicular traffic, such as a walkway or road. Due to heavy traffic and poor weather conditions, the road becomes increasingly degraded and thus threatens human safety. For this reason, automatic road anomalies detection is introduced in order to solve problems of the pavement and avoid the expensive maintenance operations. In this context, we will present in this paper two types of anomalies we have considered to achieve the main goal of our research. The first type concerns the detection of road marking degradations. To do so, we are based on our own method cited in [1] for road marking features extraction using the VIAPIX® system [2]. Indeed, relying on inverse perspective mapping technique and color segmentation to detect all white objects, our algorithm is able to examine images automatically and to provide information on road marks. Then, based on an optical correlation and a geometric recognition techniques to identify the detected objects and a technique for analyzing the state of the identified marks, it allows qualifying all road markings more accurately with a minimum of false alarms. The second type of anomalies concerns fine-structures extraction defined by our novel approach ADFD (Automatic Darkest Filament Detection) for automatic road crack detection on pavement images acquired by the Aigle-RN system [3, 4]. Indeed, our approach is composed of two main phases. Relying on the photometric characteristics, the first phase consists in selecting dark pixels that have great probability of belonging to a crack in the image. Then, based on the geometric characteristics, the second phase consists in connecting the selected dark pixels between them by applying the Dijkstra's algorithm [5] in order to get the crack skeleton in the pavement image.

Keywords: Optical correlation, Road marks, Cracks detection, Automatic method.

1. INTRODUCTION

Road anomalies detection is a challenging task which attract, since several years, the computer vision community either on the industrial or academic research field. Indeed, authorities spend time and finances to monitor the state and quality of the road pavement. In this context, many studies and surveys are made on the topic of roadway deficiencies and their impact on safety and economy. Indeed, the promise of augmented robotics technologies for tasks such as extraction of lane and road markings, automatic crack detection [6], is motivating the study of novel image processing techniques. Pavement degradation is helpful information for evaluating the road condition and conducting the necessary road maintenance. Mainly due to strong traffic and bad weather conditions [7], they can have great potential to cause catastrophic failures which can lead to huge economic loss and even serious human injury [8]. Basically, pavement anomalies detection was performed manually, which is insecure, labor-intensive and time-consuming [9]. For fast and reliable surface defect analysis, automatic detection is developed instead of the slower subjective traditional inspection procedures. Many approaches have been proposed in the past two decades. Based on the assumption that brightness along the cracks are lower than that of the background, intensity thresholding methods [10] have been extensively used for detecting cracks. As a counterpart, these methods can produce disjoint crack fragments because of the brightness inhomogeneity and the complexity of the road structure [11]. To avoid these constraints, others methods, based on the geometric shape of the cracks, have been proposed [12]. Among them, we cite the mathematical morphological approaches that have been used to reduce the discontinuities within the crack pattern and remove the false detections. However, the automation of these methods still remains difficult because of the large amount of parameters which need to be adapted. To remedy, both photometric and geometric characteristics have been exploited recently [13, 14]. In this context, the OMPS (Optimized Minimal Path Selection) method has shown to provide robust segmentation of cracks. According to [15], it has shown a superior performance in terms of accuracy and execution time on gray level pavement images. However, tests revealed

that this approach seems limited in some cases since it depends mainly on the conditions of image acquisition. For this reason, we propose in this paper our novel approach ADFD (Automatic Darkest Filament Detection) for automatic road crack detection. Based on the hypothesis that pavement cracks represent thin and dark filaments having one or more orientations, our approach aims on one side to select dark pixels that probably belong to the cracks in the image and on the other side to draw the chaotic shape of cracks by connecting the selected dark pixels between them using the Dijkstra's algorithm [5]. Before describing our approaches, we begin in section 2 by reviewing the different acquisition systems that we have used during the tests. Section 3 presents our first approach for road marking anomalies. Next, in section 4, we explain the principle of our second approach for road crack detection. Finally, we summarize in section 5 by concluding and drawing some working perspectives.

2. IMAGING SYSTEMS

2.1. VIAPIX® system

It is a vehicle-borne image-base mapping system designed for real-time image geo-referencing. A miniature inertial sensor directly merges inertial data with GPS and odometer information to optimize performance. It is composed of two modules: an acquisition module (Fig. 1(a)) to collect data from the entire road pavement and its surroundings; and an exploitation module (Fig. 1(b)) to navigate from your office in your road network and make some measurements directly on images (width, height, etc.). Once the acquisition module is installed on the roof of the car (Fig. 1(c)), it records images at regular distance intervals (set to 3 meters in the present case). These images are then transferred to the VIAPIX® exploitation module. For more details, the reader is referred to Ref. [2]. We note that this system is the one which has been used in this work in section 3 to detect the road markings.

(a) (b) (c)

Fig. 1: (a) VIAPIX® acquisition module – (b) VIAPIX® exploitation module – (c) VIAPIX® module installed on the roof of the car

2.2. Aigle-RN system

It is an imaging system developed for global inspection of the national network state. It is composed of three digital cameras filming directly the pavement. Unlike the VIAPIX® module, the sensors of this system are placed in the road environment (the optical axis is perpendicular to the road). So, once installed on the vehicle as shown in Fig. 2, it records images representing only the pavement. Images originally size 1900 × 924 pixels and cover a roadway surface of 3.80 m in with by 1 m in depth. We note that this system is the one which has been used in this work in section 4 to detect the cracks. For more details, the reader is referred to Ref. [3, 4].

Fig. 2: Aigle-RN system installed on the vehicle

3. ROAD MARKING ANOMALIES

Our proposed approach is composed of four main steps. Firstly, in order to simplify the original VIAPIX® image in a way to decrease the number of irrelevant features that do not need to be processed, the Inverse Perspective Mapping technique (IPM) is applied. Secondly, to carry out our survey, a color segmentation method based on an adaptive thresholding operation is applied in order to detect lane and road markings. Thirdly, after detecting the whole objects belonging to the road, unsupervised recognition techniques are thus performed. They consist in deciding if whether or not the detected

objects correspond to road markings. Fourthly, a final step to study and qualify the state of recognized objects, is applied. To do so, we assume that marks on the road are defined as bright objects that contrast against the road surface. As a concrete examples, our demonstration is based on the word ***"BUS"***, the ***"bikes pictograms"*** and the ***"pedestrian crossing"***.

3.1. Inverse Perspective Mapping (IPM)

This step consists in simplifying the original VIAPIX® image by reducing the number of useless features that do not need to be processed. Since our goal is to detect objects on the pavement, we note that processing the full VIAPIX® image leads to the detection of irrelevant objects, e.g., sky, buildings, cars, etc. Consequently, the key for good results is to focus on a specific area in the image. To do so, we are based on the IPM technique [16] that consists in transforming the original VIAPIX® image by an image with view from above as shown in Fig. 3.

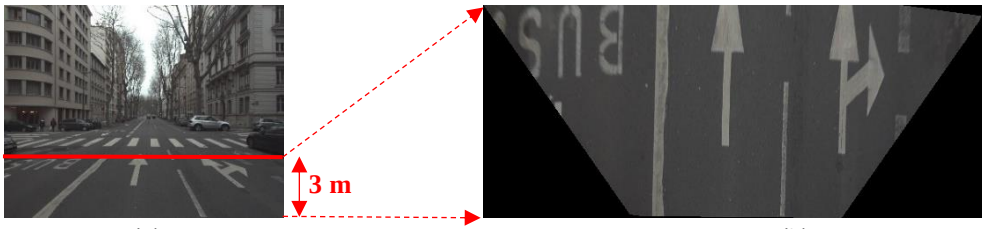

Fig. 3: (a) Example of VIAPIX® image – (b) Its IPM transformed image applied over an area of 3 m in front of the car

3.2. Detection

Since the road color changes according to the variation of the lighting conditions (shadow, rain, etc.), we propose in this study a two-steps approach that consists in detecting the lane as first step and then the road markings that belong to the detected lane as second step. For that, a thresholding operation is carried out to detect the road. For this reason, an adaptive thresholding operation based on the luminosity parameters provided by the VIAPIX® module is applied. It consists in segmenting the resulting IPM image in a manner to get the white objects that define the markings on the road.

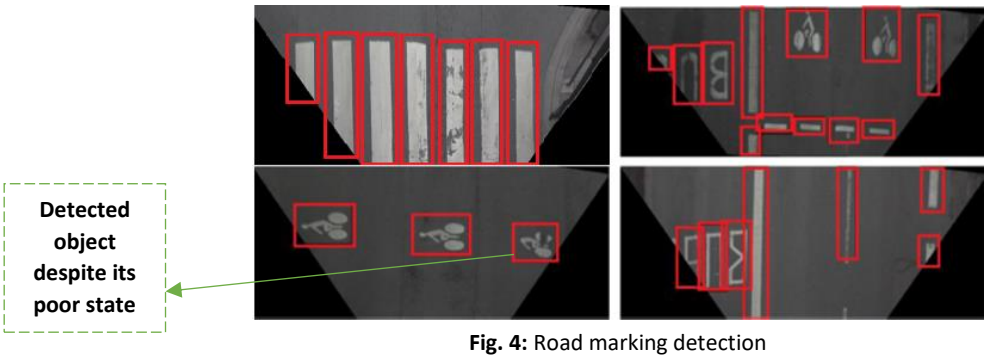

Fig. 4: Road marking detection

3.3. Recognition

a. Optical recognition technique based on optical correlation

After extracting the objects on the road, it is important to validate the detection step by a recognition step in order to identify all road markings and eliminate all false detections (needless objects). For that, we present thereafter in Fig. 5 our optical correlation technique.

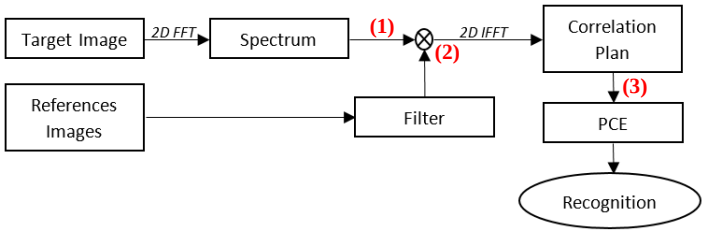

Fig. 5: Optical correlation principle

According to Fig. 5, this technique is composed of three steps. Firstly, the spectrum of the target image is computed by performing a Fast Fourier Transform (FFT). Secondly, the target image is multiplied by the correlation filter. In this work, a phase-only filter (POF) is used thanks to its good discrimination and robustness performances. Next, an Inverse Fast

Fourier Transform (IFFT) is applied. Thirdly, the Peak Correlation Energy (PCE) value defined as the energy of the peak correlation normalized with respect to the total energy in the correlation plan is computed. This value is then compared to a given threshold *'Thres'*. If the PCE is larger than *'Thres'*, the algorithm is stopped and the detected object is therefore identified. Otherwise, the object is removed since it is considered as a false alarm. Some illustrative examples for road marking recognition (the word ***"BUS"*** and the *"**bikes pictograms**"*) are shown in Fig. 6.

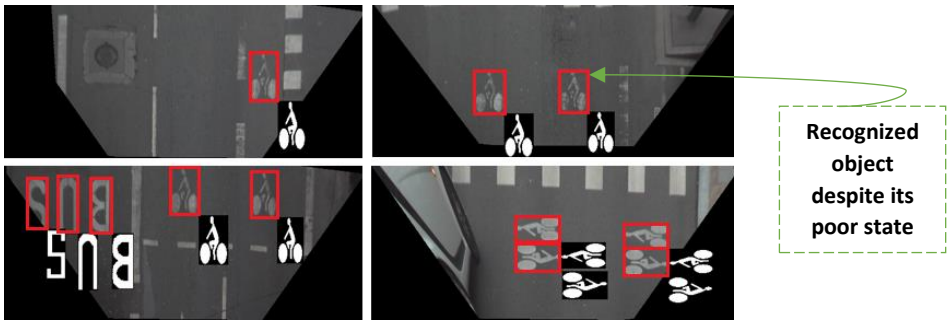

Fig. 6: Road marking identification

b. Geometric recognition technique

This technique consists in identifying the detected pedestrian crossing strips. The gist of our proposal is to specifically search for juxtaposed bright objects in the image. To do so, a three-step procedure is performed to get good detection. Firstly, the center of each object is computed (black dots in Fig. 7). Next, a series of horizontal and oriented lines (taking into account the vehicle's direction given by the VIAPIX® module) are considered. Indeed, they permit to define the extent of intervals (red lines in Fig. 7(a-b)) that may contain a pedestrian crossing (maximum of juxtaposed objects in the same interval). Finally, the third step consists in increasing the recognition rate. At this stage, juxtaposed objects which are detected in more than three successive images in the same interval, are considered as the strips of the pedestrian crossing.

(a) Horizontal intervals (b) Oriented interval (c) Identification

Fig. 7: Identified pedestrian crossing

3.4. State of the identified mark

Once the road marks are identified and their positions in different images are known, the next step of our approach consists in analyzing and qualifying their state. To do so, we proceed to calculate for each mark its length, width, area, white color level, etc. For example, a pedestrian crossing is composed of parallel white rectangular strips to the axis of the road, with a minimum length of 2.5 m in the city and 4 to 6 m in open country, a width of 0.5 m, and an inter-step distance of 0.5 m to 0.8 m. Indeed, the comparison of these standard values with those that are computed by our algorithm allows us to know roughly the state of the mark in question (good condition, average condition, bad condition).

Fig. 8: Example of identified pedestrian crossing with seven strips in the original VIAPIX® image

Table 1 : Specifics of the identified pedestrian crossing illustrated in Fig. 8

Strips number	1	2	3	4	5	6	7
Width (m)	0.51	0.48	0.51	0.50	0.49	0.51	0.48
Length (m)	2.31	3.82	4.03	3.99	3.77	3.81	3.71
Distance between two strips (m)	0.56	0.54	0.50	0.56	0.49	0.53	???
White color level	87.38	136.97	169.63	163.96	139.24	139.89	119.14

According to the computed values illustrated in Table 1, the pedestrian crossing shown in Fig. 8 is in good condition. Indeed, almost all his strips are undamaged. Therefore, there is no need to any maintenance operation in this case.

3.5. Discussions

The algorithm has been tested on several VIAPIX® images collected under varying weather and lighting conditions. All of the video sequences are captured using a 1600×1216 resolution digital camera mounted on a vehicle at a height of 1.5 m, with the speed of the vehicle varying between 30 and 50 km/h. All the performed tests indicate the good performance and accuracy of our algorithm to get information on road marks. Our concern is to generalize the algorithm to introduce a recognition and classification technique for all road markings (e.g., arrows directional, zigzag lines, handicap parking stencil, etc.) in order to qualify the general state of the marks (number of marks, their lengths, their widths, their areas, their erasure rates, etc.), check the seriousness of the marking anomaly and therefore estimate the road severity.

4. ROAD CRACK DETECTION

In this section, we detail the second part of our research package for pavement surface crack detection. For more precision, a global scheme of the proposed ADFD method is given onto Fig. 9.

Fig. 9: General synoptic of the ADFD method

According to Fig. 9, our approach can be separated in two consecutives phases from the original pavement image to the final crack skeleton detection result. The first phase consists in reducing the amount of information to be processed in the image by selecting at local scale only the dark pixels that have strong probability of belonging to a real crack on the road. Then, the second phase allows the segmentation of the one-pixel wide crack skeleton in the image. We note that the innovative aspect of this method is presented in its ability to process easily both 2D (pixel's color) and 3D (pixel's depth) pavement images.

4.1. Selection of crack Points-Of-Interest (POI)

Assuming that, on the original pavement image, the crack is darker than its surrounding, this phase permits to select locally in the image the darkest points that correspond to relevant and useful pixels, namely thereafter points-of-interest, that most likely belong to the crack pattern. To do that, the three operations shown in Fig. 10, are successively performed.

Fig. 10: Operations for the points-of-interest selection

The first operation consists in applying a global adaptive thresholding to the original pavement image. In order to not process the whole original image and thereby avoid consuming a lot of computing time, this operation acts as a pre-processing step that permits to reduce the amount of non-useful bright pixels while preserving only those that are located within dark areas. Then, a non-linear digital median filter is performed on the resulting image. Indeed, it consists in eliminating noise that might hinder the process of the crack skeleton segmentation at the next phase. In other words, the goal of this filter is to replace each dark pixel selected by the adaptive thresholding at the previous operation with the median value of the neighboring pixels. After that, to get the significant POI inside the crack pattern and thus a better crack skeleton segmentation, the filtered image is partitioned into Regions-Of-Interest (ROI) of size P×P. Among the many preserved dark pixels inside each ROI, this third operation allows retaining only the one-darkest-pixel by applying the CADP (Concentrated Area of Dark Pixels) algorithm that consists in verifying the presence of a high concentration of dark pixels within each ROI. An illustration of the POI selected in the original pavement image is shown in Fig. 11.

(a) (b)

Fig. 11: (a) A gray level Aigle-RN pavement image of 311×462 pixels – (b) The selected points-of-interest (POI)

According to Fig. 11, most of the selected POI reside within the real crack structure while few of them are located within the background texture such as those that are framed in red in Fig. 11(b).

4.2. Crack segmentation

The main goal of this phase is to refine the first extraction by estimating and analyzing the whole shape of the crack. Based on the assumption that crack corresponds to a dark and fine filament on the road, this phase aims to compute the thinnest segments between the crack points-of-interest selected at the previous phase and shown in Fig. 11(b). To do that, the two operations illustrated onto Fig. 12 are carried out.

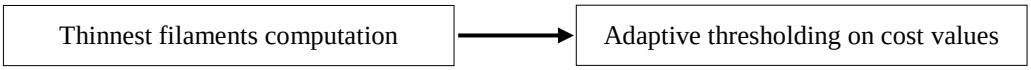

Fig. 12: Operations for the crack skeleton segmentation

Since for any observer, a crack looks, in most of time, like a chaotic trajectory having a departure and an arrival point, the first operation of this phase separates all the POI shown in Fig. 11(b) into pairs while considering them as the departures and the destinations in the process of thinnest filaments computation. In this context, the path finding strategy cited in [15] has been performed given its importance in speeding up the algorithm and its ability to avoid the repetition of the same process several times. Indeed, it consists in using 3P×2P image blocks. Thus, there are only 4 filaments to compute at the most for each central POI as shown in Fig. 13. To browse the entire pavement image, the search is then moved to the next 3P×2P image block. The four segments are computed by applying the Dijkstra's algorithm (DA) [5].

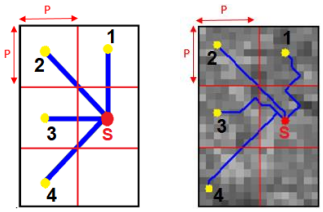

(a) (b)

Fig. 13: (a) 3P×2P strategy to browse the gray level pavement image subsets – (b) Computed thinnest filaments within one 3P×2P pavement image subset

Once the DA is applied to the all points-of-interest illustrated in Fig. 11(b), we obtain the filaments as shown in Fig. 14.

(a) (b)

Fig. 14: (a) The original gray level pavement image shown in Fig. 11(a) – (b) The thinnest filaments obtained after applying the Dijkstra' algorithm

Up to here, each of the computed filaments is characterized by a cost value defined by the average of the pixel gray level values along the filament as follows:

$$F_{sd} = \frac{1}{card(F_{sd})} \sum_{a=s}^{d} img(x_a) \tag{1}$$

where F_{sd} is the filament between the source s and destination d and x_a is a pixel of the filament in the pavement image img. Among the large set of selected filaments illustrated in Fig. 14, only a small subset are outside the real crack. Indeed, they are considered to be false detections. To remedy, the second operation shown in Fig. 12 is performed on the resulting image. According to the photometric consideration, it serves as a refining step that uses a threshold on the cost function in order to select only filaments that are inside the crack pattern. At this stage, the filaments whose cost values are lower than the threshold in eq. 2 are selected, while others are removed since they are supposed to be part of false alarms.

$$T_{cost} = \mu_{cost} - K_{cost} \times \sigma_{cost} \tag{2}$$

where μ_{cost} and σ_{cost} are the mean and the standard deviation of the filament costs, and K_{cost} is a constant which is adjusted to get a better performance.

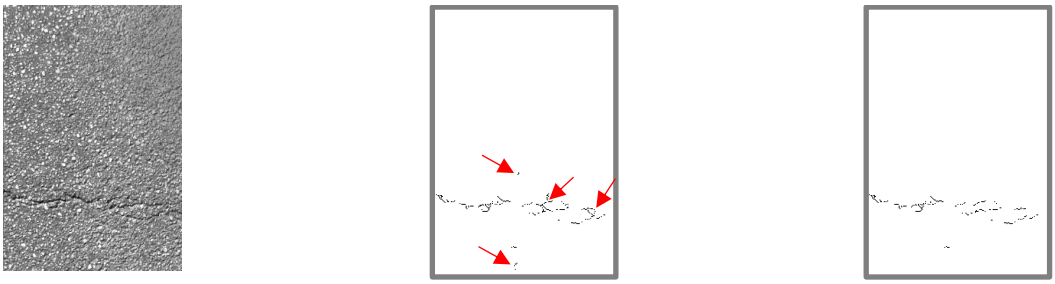

(a) (b) (c)

Fig. 15: (a) The original gray level pavement image shown in Fig. 14(a) – (b) The computed thinnest filaments shown in Fig. 14(b) – (c) The resulting crack skeleton obtained after the thresholding by T_{cost}

In comparison with the filaments shown in Fig. 14(b), the cleaning operation illustrated in Fig. 15(c) allows reducing the amount of useless vestiges that correspond to false crack detections in the image, i.e., unnecessary filaments which are pointed in red in Fig. 15(b), are withdrawn after applying the thresholding T_{cost}. Furthermore, the result of the segmentation is a set of segments that collectively cover the entire crack and draw the real crack skeleton.

4.3. Illustrative examples

According to the global process presented in section 4, we only consider the crack skeleton detection for this work. Our goal was to present the efficiency of the crack skeleton segmentation that is mainly based on the Concentrated Area of Dark Pixels and the conventional Dijkstra algorithms. Moreover, the objective was not to present a global road crack detection that is why the post-processing and the width detection steps have not been implemented for the tests shown in this paper. Consequently, for experimentation we only used the phases presented in Fig. 9. Then, to evaluate our proposed approach, we compared our obtained results with those that are obtained when applying the first three steps of the recent existing method OMPS (steps 1-3 in [15]). In this context, we have tested the algorithm on thirty three downward facing pavement images originating from the dataset available in [17] and acquired by the imaging system, namely, Aigle-RN [3, 4]. At this stage, two different datasets with images of different sizes have been used. Indeed, they have been collected at traffic speed for monitoring the roadway surface conditions of the French national network. Besides, all gray level images represent various pavement types and illustrate some typical cases and difficulties while the segmentation process. They include various types of cracks (longitudinal, transverse, combinations of longitudinal and transverse, alligator, etc.) with either thin or large cracks with or without ramifications. For the moment, the performance assessment is performed by comparing the results obtained automatically with the pseudo-ground truth (PGT) available in [17] which is considered as the reference to visually evaluate the quality of the crack skeleton segmentation. To clarify, some illustrative examples are presented in Fig. 16.

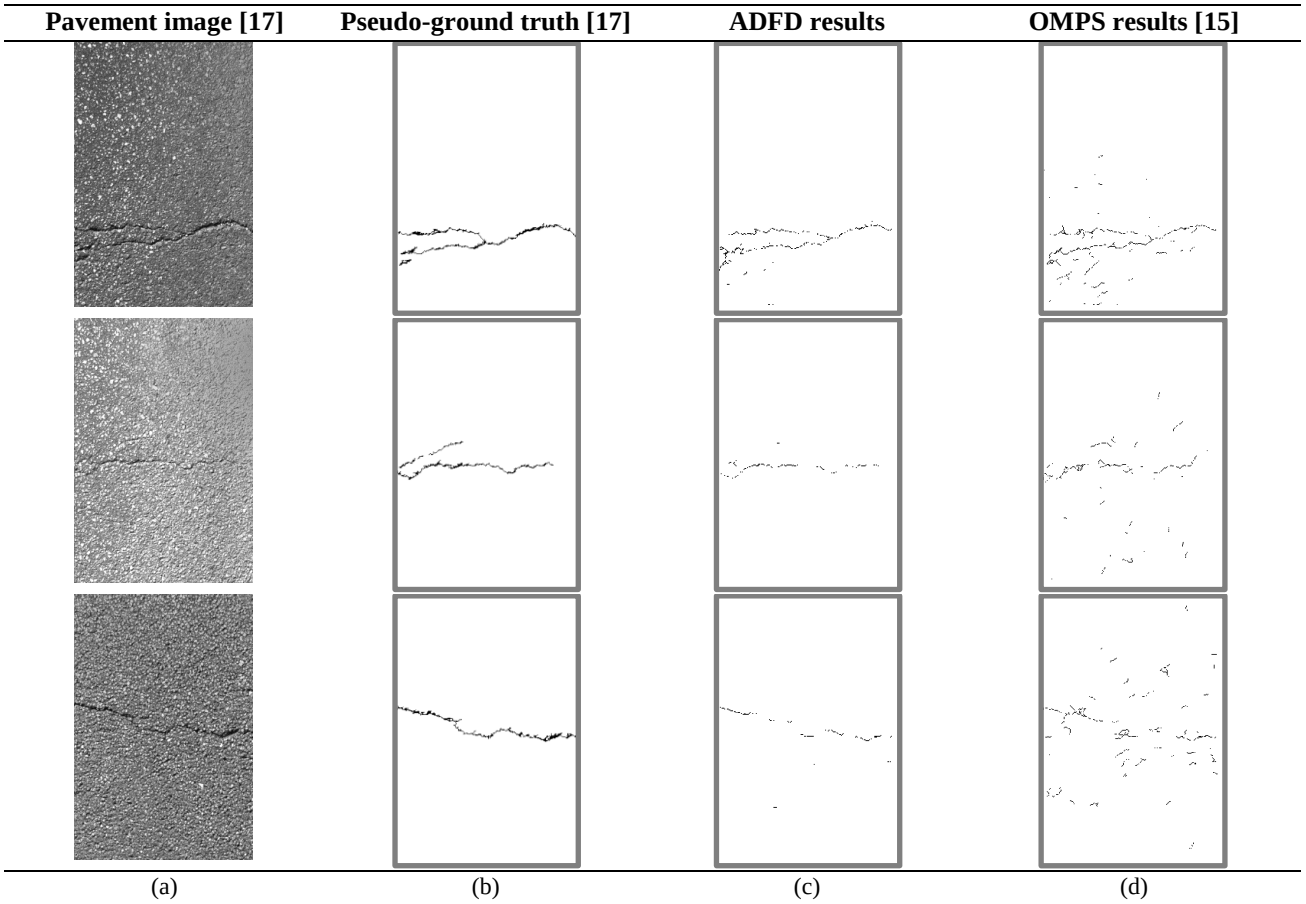

Fig. 16: Segmentation of the crack skeleton by the ADFD method vs. the OMPS method on gray level pavement images of 311×462 pixels

Fig. 16 illustrates how much we obtained best results with our proposed algorithm. Visually, the ADFD results are so close to the pseudo-ground truth with less noise according to the texture in comparison with the OMPS method which seems to be less accurate because of the large amount of artifacts scattered all around the real crack (fourth column in Fig. 16).

5. CONCLUSION AND PERSPECTIVES

This paper has presented a brief review of the ongoing tests of our approaches for automatic road anomalies detection. Firstly, a novel approach for the detection of road marking degradations is proposed and applied to several images acquired by the VIAPIX® system [2]. Based on our work cited in [1] which consists in detecting, recognizing and qualifying all the marks state on the road, our algorithm allows us to examine images rapidly and in a fully unsupervised manner. Indeed, it permits to analyze each identified object in order to study its state and thereby get a general idea about the gravity of the road. Secondly, a novel approach for automatic road crack detection is introduced. It consists in extracting the one-pixel wide crack skeleton in the image. Based on the assumption that only one filament (path) is an appropriate description of the crack, the first step of this approach consists in selecting the points-of-interest that have great probability to belong to a real crack on the road by verifying locally in the image the presence of a high density of dark pixels in a well-loaded-region. The second step permits to segment the gray level image by linking all the selected dark pixels by using the Dijkstra's algorithm.

Future work will focus on the generalization of our first approach to introduce a recognition, geolocation and classification technique for road markings with symbols (e.g., arrows directional, zigzag lines, handicap parking stencil, etc.). Another direction consists in improving our road crack detection approach by adding a post-processing step after the crack skeleton segmentation in order to further reduce the rate of false detections and thus add crack pixels that have not been detected. A final step of this work is to complete our experimentation by testing 3D images collected with the latest generation of imaging system, e.g. LCMS system [18], while taking advantage of the new information that the system can bring to us (depth of each pixel in the image).

REFERENCES

[1] Kaddah, W., Ouerhani, Y., Alfalou, A., Desthieux, M., Brosseau, C., and Gutierrez, C. Road marking features extraction using the VIAPIX® system. Optics Communications, 371, 117-127 (2016).

[2] VIAPIX® system: http://www.viapix.eu/.

[3] Cerema, Aigle-RN. www.normandie-centre.cerema.fr/IMG/pdf/15-AigleRNpress_cle243947.pdf. Accessed November (2017).

[4] Aigle-RN project: http://media.lcpc.fr/ext/pdf/sem/2008_jtr_aigle.pdf.

[5] Dijkstra, E. W., "A note on two problems in connexion with graphs", Numerische mathematik, 269-271 (1959).

[6] Kastrinaki, V., Zervakis, M., and Kalaitzakis, K., "A survey of video processing techniques for traffic applications", Image and vision computing, 21(4), 359-381 (2003).

[7] LCPC. Méthode d'essai no. 52, catalogue des dégradations de surface des chaussées, rapport général, Laboratoire Central des Ponts et Chaussées, (1998).

[8] Oliveira, H., and Correia, P. L., "Automatic road crack segmentation using entropy and image dynamic thresholding", In Signal Processing Conference, 17th European, 622-626 (2009).

[9] Nguyen, T. S., Avila, M., and Begot, S., "Automatic detection and classification of defect on road pavement using anisotropy measure", In Signal Processing Conference, 17th European, 617-621 (2009).

[10] Tsai, Y. C., Kaul, V., and Mersereau, R. M., "Critical assessment of pavement distress segmentation methods", Journal of transportation engineering, 136(1), 11-19 (2009).

[11] Zhang, L., Yang, F., Zhang, Y. D., and Zhu, Y. J., "Road crack detection using deep convolutional neural network", In Image Processing (ICIP), IEEE International Conference, 3708-3712 (2016).

[12] Subirats, P., Dumoulin, J., Legeay, V., and Barba, D., "Automation of pavement surface crack detection with a matched filtering to define the mother wavelet function used", In Signal Processing Conference, 14th European, 1-5 (2006).

[13] Shi, Y., Cui, L., Qi, Z., Meng, F., and Chen, Z., "Automatic road crack detection using random structured forests", IEEE Transactions on Intelligent Transportation Systems, 17(12), 3434-3445 (2016).

[14] Chambon, S., and Moliard, J. M., "Automatic road pavement assessment with image processing: review and comparison", International Journal of Geophysics, 2011, (2011).

[15] Kaddah, W., Elbouz, M., Ouerhani, Y., Baltazart, V., Desthieux, M., and Alfalou, A., "Optimized minimal path selection (OMPS) method for automatic and unsupervised crack segmentation within two-dimensional pavement images", The Visual Computer, 1-17 (2018) https://doi.org/10.1007/s00371-018-1515-9.

[16] Mallot, H. A., Bülthoff, H. H., Little, J. J., and Bohrer, S., "Inverse perspective mapping simplifies optical flow computation and obstacle detection", Biological cybernetics, 64(3), 177-185 (1991).

[17] Image database available: http://www.irit.fr/~Sylvie.Chambon/Crack_Detection_Database.html.

[18] LCMS system: http://www.pavemetrics.com/fr/applications-fr/inspection-des-routes/lcms-fr/.